The Impact of Sea Level Rise in the Guadiana Estuary

Lara Mills[1], João Janeiro[1] and Flávio Martins[1,2]

[1] Centro de Investigação Marinha e Ambiental (CIMA), University of Algarve, Faro, Portugal
[2] Instituto Superior de Engenharia (ISE), University of Algarve, Faro, Portugal
a60162@ualg.pt, janeiro.jm@gmail.com, fmartins@ualg.pt

Abstract. Understanding the impact of sea level rise on coastal areas is crucial as a large percentage of the population live on the coast. This study uses computational tools to examine how two major consequences of sea level rise: salt intrusion and an increase in water volume affect the hydrodynamics and flooding areas of a major estuary in the Iberian Peninsula. A 2D numerical model created with the software MOHID was used to simulate the Guadiana Estuary in different scenarios of sea level rise combined with different freshwater flow rates. An increase in salinity was found in response to an increase in mean sea level in low and intermediate freshwater flow rates. An increase in flooding areas around the estuary were also positively correlated with an increase in mean sea level.

Keywords: Guadiana Estuary, Sea Level Rise, MOHID, Salinity Intrusion

1 Introduction

A rise in mean sea level is a global concern as 10% of the world's population live within 10 meters elevation of the current sea level (Carrasco, Ferreira, & Roelvink, 2016). Based on projections by the Intergovernmental Panel on Climate Change (IPCC), the rate of sea level rise is accelerating. An acceleration in global sea level rise has been reported throughout the 20th century based on satellite altimeter data (Church & White, 2006). Global mean sea level rise could be as high as 1 meter by the year 2100 if greenhouse gas emissions continue to be very high (Church et al., 2013). As the number of people accommodating coastal areas increases, an acceleration in the rate of sea level rise will severely impact society and the economy. Impacts of sea level rise on coastal areas include submergence of land, increased flooding, increased erosion, changes in ecosystems and an increase in salinity (Nicholls et al., 2011). Not yet fully explored in the literature is how the dynamics of salinity in estuaries will evolve due to sea level rise. It is thus the aim of this work to quantify a relationship between sea level rise and salinity content in estuaries, as an increase in estuarine salinity has the potential to damage estuarine environments.

From a physical standpoint, an estuary is defined as a semi-enclosed body of water where river meets sea, extending into the river as far as the upper limit of the tides. Estuaries are productive environments, hosting highly diverse and complex ecosystems (Sampath, Boski, Loureiro, & Sousa, 2015). Fisheries, aquaculture, ecotourism and port

ICCS Camera Ready Version 2019
To cite this paper please use the final published version:
DOI: 10.1007/978-3-030-22747-0_23

facilities rely on estuaries to contribute revenues to national, regional and local economies.

These transitional areas where fresh water derived from land mixes with salt water from the sea are sensitive to changes in climate such as sea level rise. Estuaries adapt to sea level rise by deepening their channels. This increases the accommodation space of sediments, further enhancing ebb and flood asymmetry (Sampath et al., 2015).

A water column is considered stratified when less dense water lies over denser water. Thus, the stratification of an estuary is determined by the balance between buoyancy and mixing of denser salt water from the sea and less dense fresh water from land. An increase in sea level allows more salt water to enter the estuary (Ross et al., 2015). Thus, a major consequence of sea level rise in estuaries is the intrusion of salt from sea water into fresh ground water, which can further impact stratification (McLean et al., 2001).

The intrusion of salt will have a profound effect on the physical properties of estuaries as the dynamic mixing of salt water and fresh water is the driving factor regulating stratification (Ross et al., 2015). Changes in oceanic salinity combined with varying flow rates of freshwater discharge into the estuary will alter the entire estuarine circulation of salinity (Ross et al., 2015). Hong and Shen (2012) found an increase in stratification in the Chesapeake Bay as a result of an increase in salinity based on the results of a three-dimensional numerical model. This change in horizontal salinity gradients will further alter estuarine circulation and cause oxygen depletion (Hong & Shen, 2012). Alterations in estuarine circulation will be detrimental to marine ecosystems that cannot tolerate high salinity content (Chua & Xu, 2014). Furthermore, sea level rise increases salinity upstream and impacts tidal currents (Hong & Shen, 2012). A study on the impact of an increase in salinity on Louisiana estuaries by Wiseman, Swenson and Power (1990) found both positive and negative trends attributed to the variability of freshwater flow rates. These authors found that an increase in salinity results in the death or decline in the productivity of marshes, which eventually leads to land loss (Wiseman et al., 1990). Further impacts of salt intrusion include contamination of water supplies for both consumption and for the industry (Hilton, Najjar, Zhong, & Li, 2008).

The aim of this article is to present the results of a numerical model simulating salt intrusion in the Guadiana Estuary, a major estuary on the Iberian Peninsula. The model simulates different sea level rise scenarios as projected by the IPCC along with different river discharge flow rates across two different bathymetries of the estuary.

2 Methods

2.1 Study Area

The Guadiana Estuary connects the Guadiana River to the Gulf of Cadiz. The Guadiana River is the fourth longest river on the Iberian Peninsula with a length of 810 kilometers, 200 of which form a border between Portugal and Spain (Delgado et al., 2012). Beginning at its mouth in front of Vila Real de Santo António in the Algarve region of Portugal and Ayamonte, Spain, the estuary extends about 80 kilometers north to its tidal limit at Mértola. The estuary drains a total area of 66,960 km^2 (Garel, Pinto, Santos, &

ICCS Camera Ready Version 2019
To cite this paper please use the final published version:
DOI: 10.1007/978-3-030-22747-0_23

Ferreira, 2009) in front of these highly populated regions. The Guadiana Estuary is at its widest in front of Vila Real de Santo António with a width of 800 meters and is most narrow near Mértola with a width of 70 meters. The average depth of the estuary is 5 meters, but in some cases, it can reach 10 meters.

Downstream, the estuary is in the form of a submerged delta where there is moderate wave energy (Garel et al., 2009). The estuary is classified as a rock-bound estuary due to its narrow and relatively deep channel, located on a passive margin exceeding freshwater discharge (Garel et al., 2009). The Guadiana Estuary is characterized by a semi-diurnal meso-tidal regime with tidal influence 50 kilometers upstream from where it meets the Gulf of Cadiz (Delgado et al., 2012). The average neap tidal range is 1.28 meters and the average spring tidal range is 2.56 meters with a maximum spring tidal range up to 3.44 meters (Garel et al., 2009).

Tides and freshwater input control the vertical mixing and stratification of the estuary, which ranges from very well-mixed to very well-stratified (Garel et al., 2009). The mixing of the estuary varies by season, with a well-mixed water column when there is low discharge from the Guadiana River due to a lack of rainfall in the summer and a partially stratified water column in the winter when there is more discharge from the river. It is only under extreme conditions that the water column can become stratified (Basos, 2013). The ebb currents of the estuary are generally faster than flood currents, even in low river flow conditions, an effect most likely due to the large hydraulic depth of the estuarine channel. The ebb-dominance becomes more pronounced as the river discharge increases (Garel et al., 2009).

The freshwater discharge of the Guadiana River can range between 10 m^3/s and 4660 m^3/s. The construction of over 100 dams since the 1950s has controlled 70% of the drainage basin by the end of 2000 (Garel et al., 2009). Of relevance is the Alqueva Dam, located 60 kilometers from the head of the estuary. It is the largest reservoir in southern and western Europe storing 4150 hm^3 of water (Garel et al., 2009). Its closure in 2002 has significantly reduced the mean river flow from an average of 143 m^3/s over the last 26 years to 16 m^3/s after 2002 (Garel et al., 2009). Downstream the dam, the river has ephemeral flows and is dry for 40% of the year (Fortunato, Oliveira, & Alves, 2002). The Guadiana Estuary currently faces a reduction in river flow due to scarce rainfall and an increase freshwater storage.

2.2 The Model

The MOHID water modeling system was used to simulate the hydrodynamics of the Guadiana Estuary and the effects of different sea level rise scenarios on salinity distribution and transport. MOHID is a three-dimensional hydrodynamical modeling system that integrates diverse numerical models in an object-oriented programming approach (MARETEC, 2017). MOHID simulates physical and biogeochemical processes in the water column and sediments (MARETEC, 2017). MOHID water has been used to simulate the hydrodynamics of many coastal and estuarine systems, mainly the major estuaries of Portugal, but also in the Netherlands, France and Ireland (Calero Quesada et al., 2019). A recent study by Calero Quesada et al. (2019) used MOHID in 2D barotropic mode to simulate the effects of freshwater discharge and tidal forcing on tidal

ICCS Camera Ready Version 2019
To cite this paper please use the final published version:
DOI: 10.1007/978-3-030-22747-0_23

propagation in the Guadiana Estuary. This model accurately produced phase values of tidal elevations and currents as confirmed by a harmonic analysis (Calero Quesada et al., 2019). The model was able to demonstrate how freshwater discharge has a stronger effect on tidal wave amplitude upstream the estuary, whereas tidal forcing controls tidal wave amplitude downstream the estuary (Calero Quesada et al., 2019).

The finite volume method in a generic computational mesh was used to simulate hydrodynamic and salt transport models. Navier-Stokes and transport equations were solved with an Alternating Direction Implicit (ADI) method. The calculation time to stabilize the salinity field is very high when the river flow is low due to the high residency time of the estuary in low river discharge conditions. For example, with a river flow of 10 m^3/s it takes two months of simulated time for the salinity field to stabilize. The computational mesh was chosen to provide a spatial resolution appropriate for the study without incurring excessive calculation time. Thus, each simulation used a Cartesian computational mesh of 1400 x 350 cells with a constant space step of 30 meters to evaluate salinity distribution and transport as well as coastal flooding at the mouth of the Guadiana Estuary.

The model incorporates different sea level rise scenarios combined with different river discharge scenarios typical of the Guadiana River over two separate bathymetries. The first bathymetry was computed by triangular interpolation of measured bathymetric data on the mesh of 1400 x 350 cells with a space step of 30 meters. This bathymetry is indicative of the present bathymetry of the estuary and corresponds to a case in which maximum human intervention is taken to keep the coastline unchanged. The second bathymetry represents a situation in which there is no human intervention, thus allowing maximum flooding of the saltmarshes and low-lying areas. Process-based models such as MOHID cannot evaluate long-term geomorphological dynamics so the results from a behavior-oriented model by Sampath et al. (2011) were used for this specific bathymetry. The two different bathymetries are shown in figures 1 and 2.

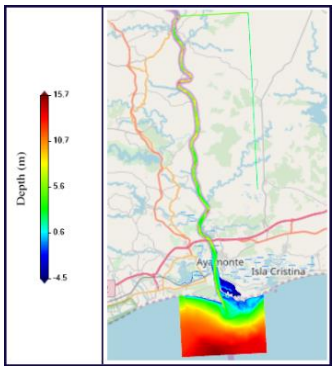

Figure 1: Computational bathymetry of the Guadiana Estuary, if the coastline is maintained (1400 x 350 cells with a space step of 30 m).

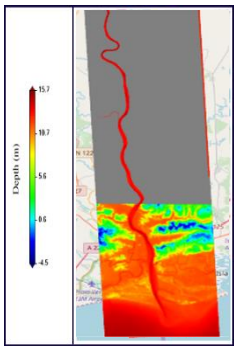

Figure 2: Computational bathymetry of the Guadiana Estuary, allowing flooding (1400 x 350 cells with a space step of 30 m). The grey area represents land.

ICCS Camera Ready Version 2019
To cite this paper please use the final published version:
DOI: 10.1007/978-3-030-22747-0_23

As previously mentioned, the flow of the Guadiana River is highly variable, so four different river discharge scenarios were simulated in the model. The first river discharge scenario of Q = 10 m^3/s represents the flow of the river in summer, when there is little rain. The second river discharge scenario of Q = 50 m^3/s and the third river discharge scenario of Q = 100 m^3/s represent intermediate conditions of the river. The fourth river discharge scenario of Q = 500 m^3/s represents a very high flow situation, which has been known to occur prior to the closure of the Alqueva Dam and will now only happen in extreme cases. A table outlining the different river discharge scenarios can be seen in table 1.

Table 1: Guadiana River freshwater discharge scenarios

Scenario	Flow Rate (m^3/s)
1	10
2	50
3	100
4	500

The model represents typical system conditions and is not associated with any specific tidal event. It was decided to force the model with an external M2 tide equivalent to the average neap and spring tide conditions, resulting in an amplitude of 1 meter.

To simulate the salinity transport in the Guadiana system, the salinity of water from the Guadiana River was considered null and the salinity of the coastal region adjacent to the estuary was set to a constant value of 36. These values are typical for this region. There are no units for salinity, in agreement with recommendations by UNESCO.

The four different river discharge scenarios mentioned above were combined with different sea level rise scenarios derived from sea level rise projections provided by the 5th IPCC report for Representative Concentration Pathway (RCP) 4.5 and RCP 8.5. Representative Concentration Pathway refers to greenhouse gas concentration (Church et al., 2013). The 5th report of the IPCC projected global mean sea level rise for these two RCP values over the years 2046-2065, 2081-2100 and the sea level rise in 2100. The mean sea level rise forecasts can be seen in table 2.

ICCS Camera Ready Version 2019
To cite this paper please use the final published version:
DOI: 10.1007/978-3-030-22747-0_23

Table 2: Predictions for the rise in global mean sea level in meters based on sea level rise from 1986-2005 for RCP 4.5 and RCP 8.5 (Adapted from the 5th IPCC Report, Church et al., 2013) and scenarios used for the present study.

		RCP 4.5	Present Study	RCP 8.5	Present Study
2046-2065	P95	0.30		0.38	
	Median.	0.26	0.24	0.30	0.24
	P05	0.19		0.22	
2081-2100	P95	0.63		0.82	0.79
	Median.	0.47	0.48	0.63	
	P05	0.32		0.45	0.48
2100	P95	0.71		0.98	
	Median.	0.53	0.48	0.74	0.79
	P05	0.36		0.52	

Due to the high computational cost of the simulations and the fact that sea level rise scenarios would be combined with the four different river discharge scenarios as shown in table 1, it became time limiting to simulate all sea level rise forecasts from the IPCC. It can be noted in table 2 that sea level rise projections overlap for the different RCP scenarios. It was decided to consider three different cases of sea level rise that covered all possibilities within all scenarios from the IPCC. The sea level rise projections used for the present study are outlined in the arrows in table 2. They correspond to a sea level rise of 0.24 m for the year 2040, 0.48 m for the year 2070 and 0.79 m for the year 2100.

The three different sea level rise projections along with the current sea level were combined with the four different river discharge scenarios along the present bathymetry of the estuary for a total of 16 simulations. Each simulation evaluated the velocity of salt transport in the Guadiana Estuary as well as areas of flooding. The flooding areas were computed along ten different classes of submersion time along a tidal cycle over the bathymetry allowing maximum flooding. Table 3 outlines the different flooding classes.

Table 3: Classes of flooding time under one tidal cycle

Class	Flood Interval In Hours
1	0 – 1.2
2	1.2 – 2.4
3	2.4 – 3.7
4	3.7 – 4.9
5	4.9 – 6.1
6	6.1 – 7.3
7	7.3 – 8.6
8	8.6 – 9.8
9	9.8 – 11.0
10	11.0 – 12.2

ICCS Camera Ready Version 2019
To cite this paper please use the final published version:
DOI: 10.1007/978-3-030-22747-0_23

For each class in table 3 the area of flooding was computed, and a histogram was constructed for the various scenarios. Flood distribution maps of four classes of inundation time: 0 to 3 hours, 3 to 6 hours, 6 to 9 hours and 9 to 12.2 hours were also constructed.

3 Results and Discussion

3.1 Temporal Evolution of Salinity

The different sea level rise and river discharge scenarios described in the methods were imposed in the model to produce several time series and horizontal distribution maps. As the number of maps and figures produced is quite high, only the results for typical system conditions are shown. The time series demonstrate the temporal evolution of salinity in several locations of the estuary over two tidal cycles for the various scenarios of sea level rise and different freshwater flow rates. The locations used for each time series can be seen in figure 3.

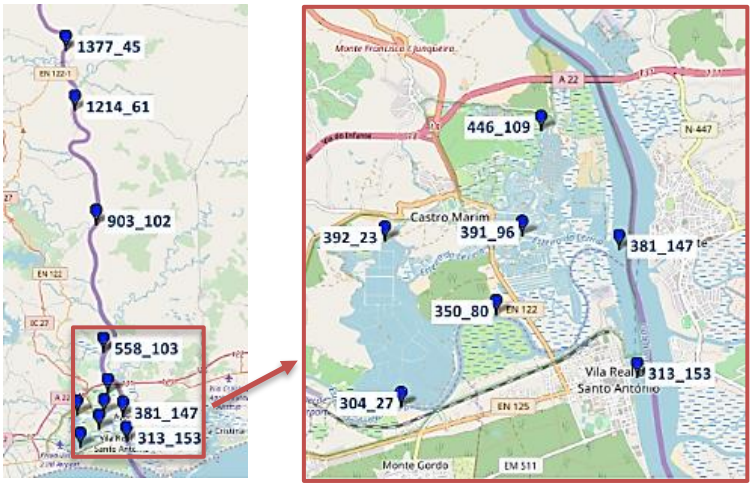

Figure 3: Location and nomenclature of points used in the time series

The time series showed an increase in salinity in response to mean sea level rise in the main channel and lower area of the estuary for low river discharge flow rates (10 m^3/s) in the present bathymetry. The results for locations further upstream depicted an increase in salinity at both low and high tide, with salinity differences of approximately 6.

The velocity time series showed a reduction in advective transport at the mouth of the estuary due to mean sea level rise. Salt is transported mainly by diffusion, in the innermost regions where the signal of the tide is not detected. This result is consistent with other values of velocity obtained for this region. Further upstream the estuary, the salinity increased to about 4 in response to an increase in mean sea level. The increase

ICCS Camera Ready Version 2019
To cite this paper please use the final published version:
DOI: 10.1007/978-3-030-22747-0_23

in salinity in response to an increase in mean sea level is more pronounced closer to the coastline than it is upstream the main channel.

The time series results are similar for intermediate discharge flows (50 m^3/s) with an increase in salinity followed by an increase in mean sea level. However, the salinity differences are much less pronounced with a salinity increase of 2 in the main channel. At the streams that let out into the estuary, the salinity decreased to a value of 4, most likely due to the increase in water volume during ebb periods.

The salinity changes were much less pronounced for higher flow rates (100 m^3/s and 500 m^3/s) as the entire system is dominated by fresh water from the main channel. Velocity time series for a river discharge of 10 m^3/s and 100 m^3/s downstream the estuary and in the main channel are shown in figures 4 and 5. Salinity time series for a river discharge of 10 m^3/s and 100 m^3/s are shown in figures 6 and 7.

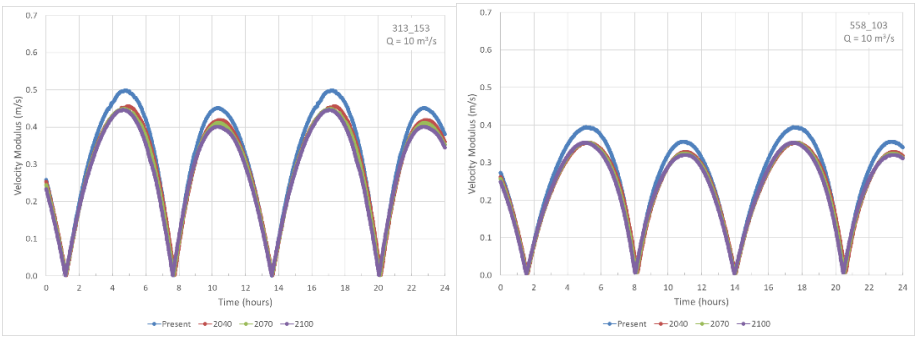

Figure 4: Velocity time series over two tidal cycles for a river discharge of 10 m^3/s in the various scenarios of sea level rise downstream the estuary (left) and in the main channel (right).

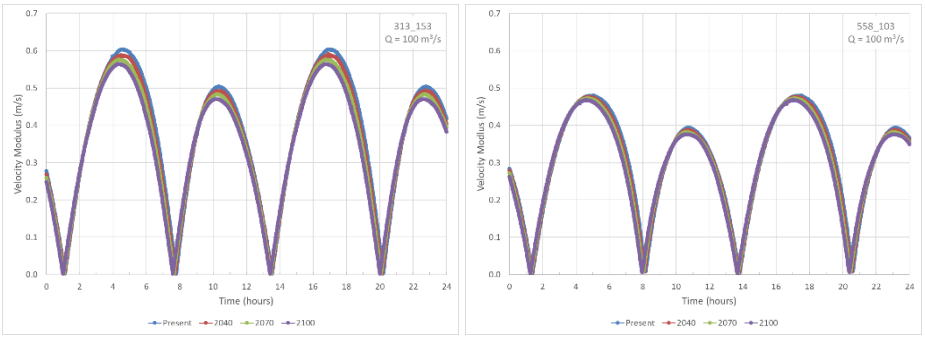

Figure 5: Velocity time series over two tidal cycles for a river discharge of 100 m^3/s in the various scenarios of sea level rise downstream the estuary (left) and in the main channel (right).

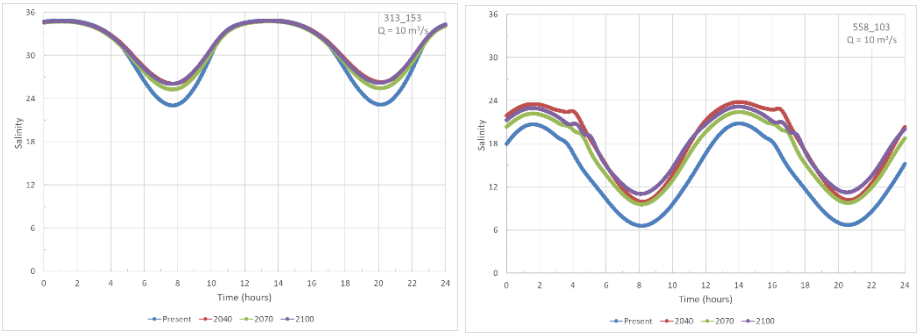

Figure 6: Salinity time series over two tidal cycles for a river discharge of 10 m^3/s in the various scenarios of sea level rise downstream the estuary (left) and in the main channel (right).

ICCS Camera Ready Version 2019
To cite this paper please use the final published version:
DOI: 10.1007/978-3-030-22747-0_23

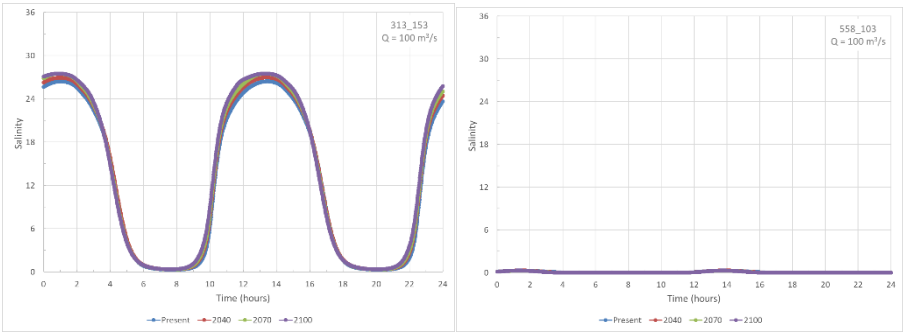

Figure 7: Salinity time series over two tidal cycles for a river discharge of 100 m^3/s in the various scenarios of sea level rise downstream the estuary (left) and in the main channel (right).

3.2 Horizontal Distribution of Salinity Transport

The salinity distribution maps for the present bathymetry in high water conditions for the different scenarios of sea level rise can be seen in figures 8 and 9. Figures 10 and 11 show the salinity distribution maps for the present bathymetry in low water conditions. Only salinity maps for a river discharge of 10 m^3/s and 100 m^3/s are shown as they are most representative of typical system conditions.

For scenarios with low freshwater discharge flow (10 m^3/s) and at high tide, the salinity progresses upstream in response to sea level rise in the main channel. At the intersection of the main channel and Carresqueira and Lezíria where the salinity has a value of 20, salinity progresses about 3100 meters upstream from the present situation to the year 2040. The salinity intrusion after the year 2040 continues to progress upstream, but at a much slower rate.

The evolution of salinity at the mouth of the estuary is less dramatic as mentioned in the time series analysis, but salinity intrusion can evolve by tens or hundreds of meters.

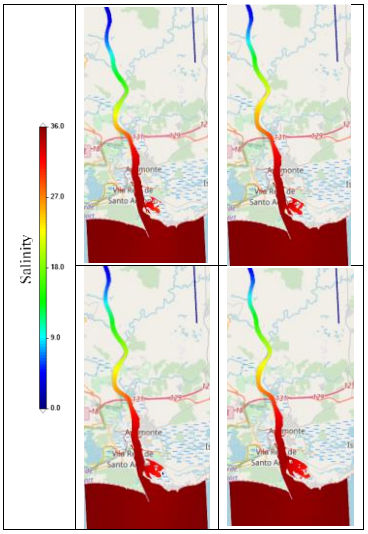

Figure 8: Salinity distribution maps in high water conditions for a discharge flow of 10 m^3/s for the present year, 2040, 2070 and 2100.

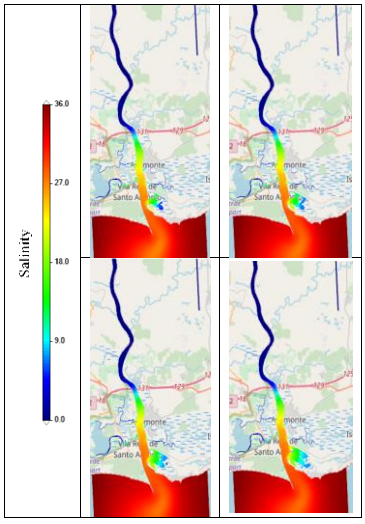

Figure 9: Salinity distribution maps in high water conditions for a discharge flow of 100 m^3/s for the present year, 2040, 2070 and 2100.

ICCS Camera Ready Version 2019
To cite this paper please use the final published version:
DOI: 10.1007/978-3-030-22747-0_23

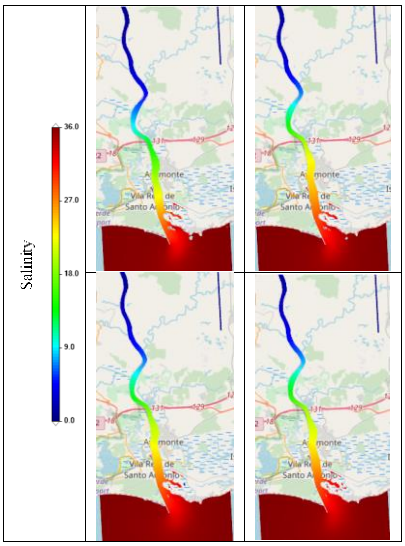

Figure 10: Salinity distribution maps in low water conditions for a discharge flow of 10m^3/s for the present year, 2040, 2070 and 2100.

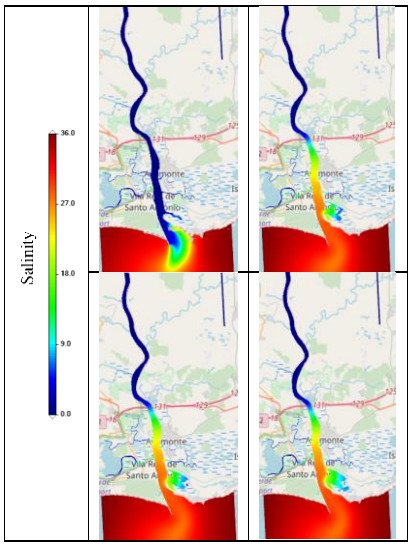

Figure 11: Salinity distribution maps in low water conditions for a discharge flow of 100m^3/s for the present year, 2040, 2070 and 2100.

3.3 Areas of Flooding

Flooding area was computed as a function of the number of hours of submersion over one tidal cycle in the various scenarios of sea level rise as shown in table 4. The analysis was carried out for the scenario of the highest freshwater discharge (500 m^3/s). Areas located further downstream the estuary are not as affected by the mean sea level rise combined with a high flow rate compared to areas located upstream. This is evident in the flood distribution map in figure 13.

The results depict an increase in submerged land area with an increase in mean sea level. The total intertidal submersion area increases from a value of 10 km^2 for the present year to a value of 14 km^2 in the “2100” scenario. The relationship between mean sea level and flooding area is nearly linear. Furthermore, an increase in mean sea level corresponds to a higher submersion time. For example, the present scenario is class 4 (3.7 to 4.9 hours of submersion), but the “2100” scenario is class 6 (6.1 to 7.3 hours of submersion). Figures 13 and 14 show the flooded regions over the various sea level rise scenarios by class of submersion time. The evolution of the inundated area is more pronounced in the north margin of the inlet not confined by Vila Real de Santo António. The marshes near the terminal section of Ribeira do Beliche also suffer high inundation areas as a result of sea level rise. The present study does not have bathymetry data for locations further upstream this point, so no conclusions can be drawn for the flooding areas upstream. Since the river has a narrower upstream profile the areas of flooding are expected to be lower.

ICCS Camera Ready Version 2019
To cite this paper please use the final published version:
DOI: 10.1007/978-3-030-22747-0_23

Table 4: Flood distribution areas based on hours of submersion over one tidal cycle in the various scenarios of sea level rise.

Class	Hours of Submersion	Area (km^2)			
		Present	2040	2070	2100
1	0 – 1.2	0.57	0.56	0.60	0.59
2	1.2 – 2.4	1.39	1.45	1.65	1.45
3	2.4 – 3.7	1.46	1.59	1.54	1.86
4	3.7 – 4.9	1.82	1.93	2.04	2.11
5	4.9 – 6.1	1.19	1.63	1.69	1.86
6	6.1 – 7.3	1.29	1.46	1.97	2.17
7	7.3 – 8.6	0.81	1.03	1.18	1.38
8	8.6 – 9.8	0.82	0.99	0.97	1.22
9	9.8 - 11	0.63	0.54	0.72	0.85
10	11 – 12.2	0.24	0.24	0.31	0.44
	Total	**10.23**	**11.41**	**12.67**	**13.93**

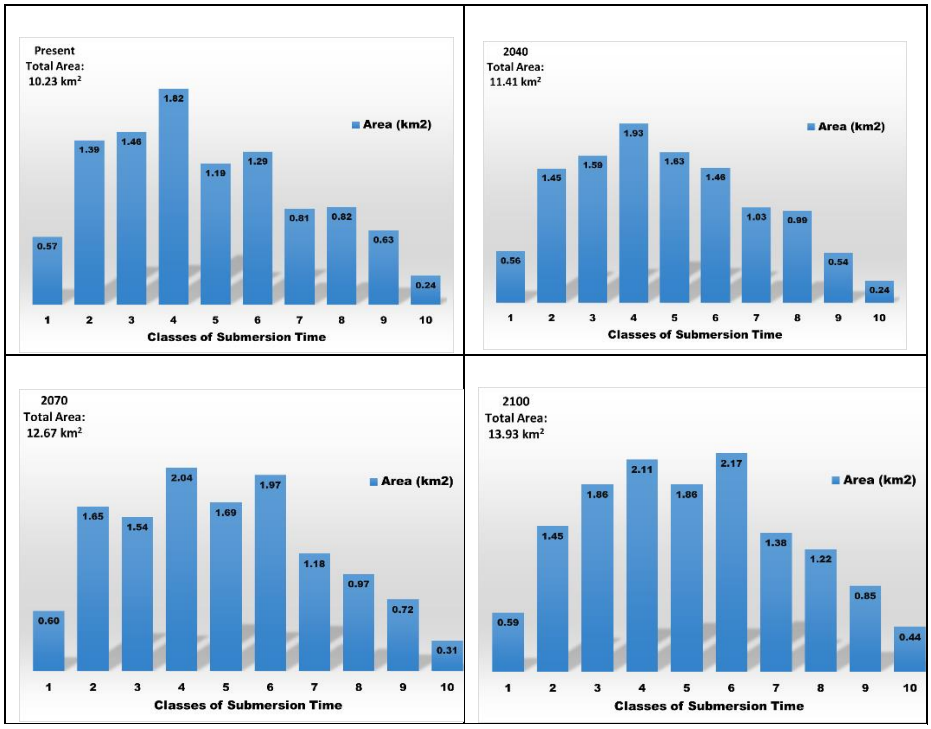

Figure 12: Histogram of flood distribution areas as a function of the number of hours of immersion over one tidal cycle in the various scenarios of sea level rise.

ICCS Camera Ready Version 2019
To cite this paper please use the final published version:
DOI: 10.1007/978-3-030-22747-0_23

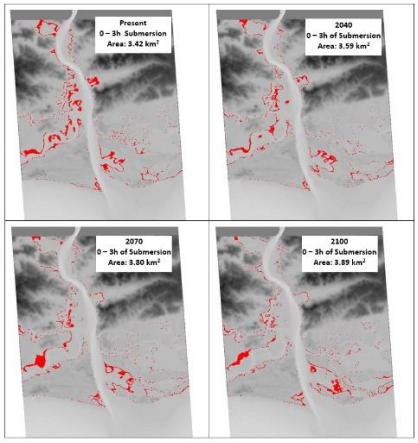

Figure 13: Distribution maps of flooded areas after 0 to3 hours of immersion over one tidal cycle in the various scenarios of sea level rise

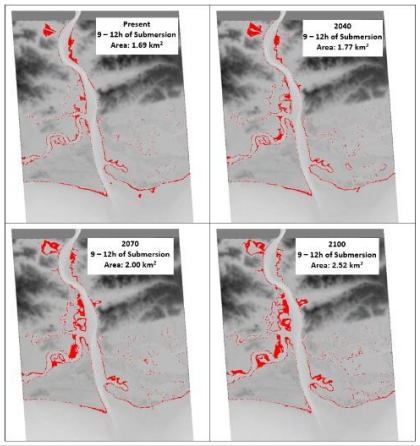

Figure 14: Distribution maps of flooded areas after 9 to 12 hours of immersion along a tidal cycle in the various scenarios of sea level rise.

4 Conclusion

This study used a numerical model to analyze several impacts of sea level rise in the Guadiana Estuary. Sea level rise projections obtained from the 5th report of the IPCC for RCP 4.5 and RCP 8.5 scenarios for the years 2040, 2070 and 2100 were imposed in the model to simulate three different scenarios of sea level rise. The parameters of the simulations allowed an analysis of the velocity modulus, salinity and flooding areas of the Guadiana Estuary.

The model demonstrated that an increase in mean sea level generally results in a decrease in the velocity modulus of the main channel of the estuary. This is most likely due to the increase in depth of the main channel as well as an increase in water volume associated with the rise in mean sea level.

The model simulations demonstrated that the mixing and transport of salinity is the result of a complex dynamic in which the lower portion of the Guadiana Estuary is dependent on both freshwater flow from the Guadiana River and the mean sea level of the adjacent coastal waters. The Guadiana Estuary alternates between purely fresh water when there is a high discharge from the Guadiana River and water of varying salinities for intermediate or low flows from the river. In the latter situation, the tide dominates the salinity with a semi-diurnal pattern.

For lower freshwater discharge rates, salinity increased in response to an increase in mean sea level with a more pronounced change in salinity in the main channel. For intermediate discharge flows, the increase in water volume due to sea level rise induced a higher penetration of fresh water from the outlet and therefore resulted in lower salinity values at the mouth of the estuary. For high discharge flows only fresh water was observed in all locations of the estuary. The results of the flood distribution areas

ICCS Camera Ready Version 2019
To cite this paper please use the final published version:
DOI: 10.1007/978-3-030-22747-0_23

demonstrated an increase in submerged land area due to mean sea level rise with an estimated increase of 4 km^2 for the entire intertidal area of the present situation. There is most significant flooding at Esteiro da Carrasqueira and the marshland surrounding Ribeira de Beliche.

The results portray an overall increase in both salinity and flooding area in the Guadiana Estuary with respect to an increase in mean sea level. As these two consequences are detrimental to estuarine ecosystems, society and the economy, further research must be done to further analyze the impacts of sea level rise in the Guadiana Estuary. One limitation of this study is that a two-dimensional model was used as opposed to a three-dimensional model. It is representative of most cases of the Guadiana Estuary because it is generally well-mixed, but as previously mentioned the estuary can become partially stratified in high freshwater flow conditions. A three-dimensional model could provide a more complete analysis of the hydrodynamics of the estuary. Additional numerical models should be simulated to portray a more quantifiable relationship between salinity and sea level rise and to further examine how the salinity changes with respect to other parameters, such as different tidal ranges.

References

1. Basos, N. (2013). *GIS as a tool to aid pre- and post-processing of hydrodynamic models . Application to the Guadiana Estuary Faculdade de Ciências e Tecnologia e Instituto Superior de Engenharia GIS as a tool to aid pre- and post-processing of hydrodynamic models . Applica*. Faro, Portugal.
2. Calero Quesada, M. C., García-Lafuente, J., Garel, E., Delgado Cabello, J., Martins, F., & Moreno-Navas, J. (2019). Effects of tidal and river discharge forcings on tidal propagation along the Guadiana Estuary. *Journal of Sea Research*, *146*(January), 1–13. https://doi.org/10.1016/j.seares.2019.01.006
3. Carrasco, A. R., Ferreira, O., & Roelvink, D. (2016). Coastal lagoons and rising sea level: A review. *Earth-Science Reviews*, *154*, 356–368. https://doi.org/10.1016/j.earscirev.2015.11.007
4. Chua, V. P., & Xu, M. (2014). Impacts of sea-level rise on estuarine circulation: An idealized estuary and San Francisco Bay. *Journal of Marine Systems*, *139*, 58–67. https://doi.org/10.1016/j.jmarsys.2014.05.012
5. Church, J. A., Clark, P. U., Cazenave, A., Gregory, J. M., Jevrejeva, S., Levermann, A., … Unnikrishnan, A. S. (2013). 2013: Sea level change. *Climate Change 2013: The Physical Science Basis. Contribution of Working Group I to the Fifth Assessment Report of the Intergovernmental Panel on Climate Change*, 1137–1216. https://doi.org/10.1017/CB09781107415315.026
6. Church, J. A., & White, N. J. (2006). A 20th century acceleration in global sea-level rise. *Geophysical Research Letters*, *33*(1), 94–97. https://doi.org/10.1029/2005GL024826
7. Delgado, J., Boski, T., Nieto, J. M., Pereira, L., Moura, D., Gomes, A., …

ICCS Camera Ready Version 2019
To cite this paper please use the final published version:
DOI: 10.1007/978-3-030-22747-0_23

García-Tenorio, R. (2012). Sea-level rise and anthropogenic activities recorded in the late Pleistocene/Holocene sedimentary infill of the Guadiana Estuary (SW Iberia). *Quaternary Science Reviews*, *33*, 121–141. https://doi.org/10.1016/j.quascirev.2011.12.002

8. Fortunato, A. B., Oliveira, A., & Alves, E. T. (2002). Circulation and Salinity Intrusion in the Guadiana estuary (Portugal/Spain). *Thalassas*, *18(2)*(December 2015), 43–65.
9. Garel, E., Pinto, L., Santos, A., & Ferreira, Ó. (2009). Tidal and river discharge forcing upon water and sediment circulation at a rock-bound estuary (Guadiana estuary, Portugal). *Estuarine, Coastal and Shelf Science*, *84*(2), 269–281. https://doi.org/10.1016/j.ecss.2009.07.002
10. Hilton, T. W., Najjar, R. G., Zhong, L., & Li, M. (2008). Is there a signal of sea-level rise in Chesapeake Bay salinity? *Journal of Geophysical Research: Oceans*, *113*(9), 1–12. https://doi.org/10.1029/2007JC004247
11. Hong, B., & Shen, J. (2012). Responses of estuarine salinity and transport processes to potential future sea-level rise in the Chesapeake Bay. *Estuarine, Coastal and Shelf Science*, *104–105*, 33–45. https://doi.org/10.1016/j.ecss.2012.03.014
12. MARETEC. (2017). MOHID Water. Retrieved April 4, 2019, from http://wiki.mohid.com/index.php?title=Mohid_Water
13. McLean, R. F., Tsyban, A., Burkett, V., Codignott, J. O., Forbes, D. L., Mimura, N., … Ittekkot, V. (2001). Coastal Zones and Marine Ecosystems. *Climate Change 2001: Impacts, Adaptation and Vulnerability*, pp. 343–379. Cambridge, UK.
14. Nicholls, R. J., Marinova, N., Lowe, J. A., Brown, S., Vellinga, P., De Gusmão, D., … Tol, R. S. J. (2011). Sea-level rise and its possible impacts given a "beyond 4°C world" in the twenty-first century. *Philosophical Transactions of the Royal Society A: Mathematical, Physical and Engineering Sciences*, *369*(1934), 161–181. https://doi.org/10.1098/rsta.2010.0291
15. Ross, A. C., Najjar, R. G., Li, M., Mann, M. E., Ford, S. E., & Katz, B. (2015). Sea-level rise and other influences on decadal-scale salinity variability in a coastal plain estuary. *Estuarine, Coastal and Shelf Science*, *157*, 79–92. https://doi.org/10.1016/j.ecss.2015.01.022
16. Sampath, D. M. R., Boski, T., Loureiro, C., & Sousa, C. (2015). Modelling of estuarine response to sea-level rise during the Holocene: Application to the Guadiana Estuary-SW Iberia. *Geomorphology*, *232*, 47–64. https://doi.org/10.1016/j.geomorph.2014.12.037
17. Sampath, D. M. R., Boski, T., Silva, P. L., & Martins, F. A. (2011). Morphological evolution of the Guadiana estuary and intertidal zone in response to projected sea-level rise and sediment supply scenarios. *Journal of Quaternary Science*, *26*(2), 156–170. https://doi.org/10.1002/jqs.1434
18. Wiseman, W. J., Swenson, E. M., & Power, J. (1990). Trends in Louisiana Estuaries Salinity. *Estuaries*, *13*(3), 265–271.

ICCS Camera Ready Version 2019
To cite this paper please use the final published version:
DOI: 10.1007/978-3-030-22747-0_23